Detection and analysis of short-period geomagnetic perturbations during increased solar activity and magnetic storms

Oksana Mandrikova[1,2*], *Igor Solovev*[1], *Alexander Zaitsev*[3]

[1]Institute of Cosmophysical Research and Radio Wave Propagation FEB RAS, 684034 Kamchatka region, Elizovskiy district, Paratunka, Mirnaya str., 7, Russia
[2]Kamchatka State Technical University, 683003 Kamchatka region, Petropavlovsk-Kamchatskiy, Kluchevskaya st., 35, Russia
[3]Institute of Terrestrial Magnetism, Ionosphere and Radio Wave Propagation named after Nikolay Pushkov of the RAS, 142191, Moscow Oblast, Troitsk, Ulitsa Tekstilshchikov st., 1b, Russia

Abstract. The dynamics of geomagnetic field variations on the eve and during the periods of magnetic storms of 2015 and 2017 has been studied (data of the horizontal component of the Earth's magnetic field of the terrestrial station network were used). The method developed by the authors based on wavelet transform and adaptive threshold functions was applied. Weak geomagnetic disturbances synchronously appearing at the stations and preceding the onset of strong magnetic storms was extracted. The correlation of the isolated geomagnetic disturbances with the AE-index is shown, both in the occurrence times and in intensities. On the basis of comparison with interplanetary environment data (interplanetary magnetic field data and the solar wind parameters were analyzed), and also based on the results of other author works [1, 2]. we assume that the isolated effects have solar nature. The research is supported by the grant of the Russian Science Foundation No. 14-11-00194.

1 Introduction

The work is aimed at developing methods for analyzing geomagnetic data and studying the processes in the magnetosphere during perturbed periods. The complexity of processing and analysis of geomagnetic data is associated with their complex nonstationary structure, with the presence of local features of different amplitude and duration. These features contain important information about the occurring processes in the magnetosphere. The use of traditional methods and approaches does not allow us to research the rapidly-variable structure of geomagnetic field variations in detail and leads to the loss of meaningful information. One of the most effective modern methods of data analysis is the wavelet transform [3-8].The wavelet transform is now successfully used for the tasks of denoising the geomagnetic data [4, 6, 8], extraction of the periodic components caused by the Earth's rotation [4 ,8], search for the precursors of intense solar flares [3], automatic detection of

* Corresponding author: oksanam1@mail.ru

magnetic storm development [8], studying of the characteristics of solar daily variations based on data from ground-based magnetic stations [7], automation of geomagnetic activity indices calculation such as K-index [9, 10], Dst-index and wavelet based index of storm activity «WISA» [4, 8] as well as several other issues. This mathematical apparatus is taken as the basis for the study.

Earlier, the authors in the works [9, 10] proposed a geomagnetic field variation model (FVM) based on wavelets. It allows describing both the characteristic variations and nonstationary short-period changes characterizing fast processes in the magnetosphere. On the basis of the FVM, computational algorithms for isolation and evaluation of local variations [11, 12] have been developed, which allow us to study short-period small-scale (from a few seconds to tens of minutes) geomagnetic field parameters in detail. Application of these algorithms allowed us to extract anomalous changes in field variations (the data of meridionally located stations was used) arising on the eve and during magnetic storms [11-13]. This study is a continuation of the previous works. The paper presents the results of data processing and analysis from a geomagnetic station network in the northeast of Russia (Yakutsk «YAK», Magadan «MGD», Paratunka «PET», Khabarovsk «KHB») and from an equatorial station (Guam «GUA», USA). The results of the work confirmed the possibility of synchronous appearance of weak geomagnetic perturbations preceding the onset of strong magnetic storms. On the basis of data comparison with of the interplanetary environment parameters (the interplanetary magnetic field data and the solar wind parameters were analyzed), and also based on the results of other author works [1, 2], we assume that isolated effects have solar nature.

2 Description of the method

The geomagnetic field variation can be represented as a combination of functions [9, 14]:

$$f(t) = f_{trend}(t) + f_{pert}(t) + e(t) = \sum_n c_{m,n}\varphi_{m,n}(t) + \sum_{j\in I} g_j(t) + e(t), \qquad (1)$$

where the component $f_{trend}(t) = \sum_n c_{m,n}\varphi_{m,n}(t)$ describes the geomagnetic field variations during quiet periods, $\varphi_m = \{\varphi_{m,n}\}_{n\in Z}$ is the basis of the smoothing scaling function, the coefficients $c_{m,n} = \langle f, \varphi_{m,n}\rangle$, m is the scale level of decomposition; component $f_{pert}(t) = \sum_{j\in I}\sum_n d_{j,n}\Psi_{j,n}(t)$ describes geomagnetic perturbations that occur during periods of increasing geomagnetic activity, coefficients $d_{j,n} = \langle f, \Psi_{j,n}\rangle$, $\Psi_j = \{\Psi_{j,n}\}_{n\in Z}$ are the wavelet basis, I is a set of indices, j is the scale parameter; component $e(t)$ is noise.

The representation (1) will be called the geomagnetic field variation model (FVM). The method for identifying the model component f_{trend} (see Equations (1)) is described in [9, 14]. The results of the method application for the «Paratunka» station (Kamchatka Region) data are given in the works [9-12], which show that

$$f_{trend}(t) = \sum_n c_{-6,n}\varphi_{-6,n}(t),$$

where $\varphi_{-6} = \{\varphi_{-6,n}\}_{n\in Z}$ is the basis for smoothing the scaling function of the 6th scale level decomposition, coefficients $c_{-6,n} = \langle f, \varphi_{-6,n}\rangle$. As an approximating basis, the Daubechies basis of order 3 is used, which was determined by minimizing the approximation error.

On the basis of the component f_{trend}, the authors developed a method for calculating the geomagnetic activity indices K, which makes it possible to reproduce the method of J. Bartels for the first time in an automatic mode [9, 10]. In this work, the component f_{trend} is not used.

To identify the set of indices I defining the model component f_{pert} (see Equations (1)), a criterion was proposed [15]:

$$j \in I \text{, if } m(A_j^v) > m(A_j^k) + \varepsilon \text{,} \tag{2}$$

where $A_j^k = \left| d_{j,k} \right|$, m is the sample average, v is the index of perturbed field variation, k is the index of quiet field variation, ε is the some small positive number.

Assuming A_j^k is normally distributed with some mean μ^k and variance $\sigma^{2,k}$, it is possible to estimate ε as $\hat{\varepsilon} = x_{\frac{1-\alpha}{2}} \sqrt{\sigma^{2,k}}$, where $x_{\frac{1-\alpha}{2}}$ is the $\frac{1-\alpha}{2}$ quantile of the standard normal distribution [9].

Since A_j^k in (2) characterizes the magnitude of the deviation of a function from its characteristic level on a scale j at time $t = k$ [16], it is taken as a measure of magnetic disturbance on a scale j at a time $t = k$. Then we get the following representation of the FVM [14]:

$$\begin{aligned} f(t) &= f_{trend}(t) + \sum_{j,n} F_0(d_{j,n}) \Psi_{j,n}(t) + \sum_{j,n} F_1(d_{j,n}) \Psi_{j,n}(t) + \\ &+ \sum_{j,n} F_2(d_{j,n}) \Psi_{j,n}(t) + e(t) = f_{trend}(t) + g^+(t) + g^-(t) + e(t) \end{aligned} \tag{3}$$

$$F_0(x) = \begin{cases} x, if \left| x \right| < T_j \\ 0, if \left| x \right| \geq T_j \end{cases}, \; F_1(x) = \begin{cases} 0, if \; x < T_j \\ x, if \; x \geq T_j \end{cases}, \; F_2(x) = \begin{cases} 0, if \; x > -T_j \\ x, if \; x \leq -T_j \end{cases} \tag{4}$$

where component $g^+(t) = \sum_{j,n} F_1(d_{j,n}) \Psi_{j,n}(t)$ describes positive increases in geomagnetic activity, component $g^-(t) = \sum_{j,n} F_2(d_{j,n}) \Psi_{j,n}(t)$ describes negative increases in geomagnetic activity. Coefficients $d_{j,n}$, for which $\left| d_{j,n} \right| < T_j$, we consider to be noise.

Considering the essential nonstationarity of the functions $g^+(t)$ and $g^-(t)$ in the representation (3), adaptive thresholds $T_j = T_j^{ad}$ are introduced for their identification (see Equations (4)) [12]:

$$T_j^{ad} = U * St_j \tag{6}$$

where $U -$ is the threshold coefficient, $St_{j_t} = \sqrt{\frac{1}{l-1} \sum_{k=1}^{l} \left(d_{j,n} - \overline{d_{j,n}} \right)^2}$, $\overline{d_{j,n}}$ is the average value, calculated in the gliding window of duration l. Window duration l and threshold coefficient U determine the size of the time window within which assess perturbations and the intensity of detected geomagnetic perturbations, respectively.

Considering that value $A_j^k = \left| d_{j,k} \right|$ is a measure of magnetic perturbations on the scale j at the time $t = k$, the intensity of positive (I_k^+) and negative (I_k^-) perturbations of geomagnetic field at the time moment $t = k$ can be determined as

$$I_k^{+-} = \sum_{j_{pert}} \left| d_{j_{pert},k}^{+-} \right|. \quad (6)$$

3 Experimental results and discussion

In the work, the geomagnetic data of minute resolution from the Russia's Northeast stations network and from the equatorial station GUA were processed (see Table 1 and Figure 1). In order to analyze geomagnetic perturbations in the auroral zone, we used the index of auroral electrojet (AE) (http://isgi.unistra.fr). Calculation of the AE index is based on the data of stations located in auroral and subauroral latitudes [17]. In order to analyze the equatorial current system, we used the Dst index (http://wdc.kugi.kyoto-u.ac.jp/dst_final/index.html), which is calculated using the data from the stations located near the Equator [18]. The results of our analysis were compared with the data of interplanetary magnetic field (IMF) and the solar wind parameters (http://www.srl.caltech.edu/ACE/ASC/index.html). The results of data processing during the magnetic storm on May 27, 2017 and July 16, 2017 are presented below in detail.

Table 1. Observatories whose data were used

Observatory	IAGA code	Geographical latitude (N)	Geographical longitude (E)	Geomagnetic latitude (N)*	Geomagnetic longitude (E)*	Local time (LT)
Yakutsk	YAK	$62^0$02.1’	$129^0$42.1’	$52^0$26.4’	$163^0$13’	UTC+09
Magadan	MGD	$59^0$33.1’	$150^0$48.3’	$51^0$32.4’	$146^0$2.4’	UTC+11
Paratunka	PET	$52^0$58.3’	$158^0$15.0’	$45^0$51.6’	$137^0$57.6’	UTC+12
Khabarovsk	KHB	$48^0$29.0’	$135^0$04.0’	$39^0$15’	$15^0$48.6’	UTC+10
Guam, USA	GUA	$11^0$22.0’	$145^0$35.0’	$3^0$73’	142^0 34’	UTC+10

*Geomagnetic coordinates were calculated using the IGRF model [19] (http://wdc.kugi.kyoto-u.ac.jp/igrf/gggm/index.html).

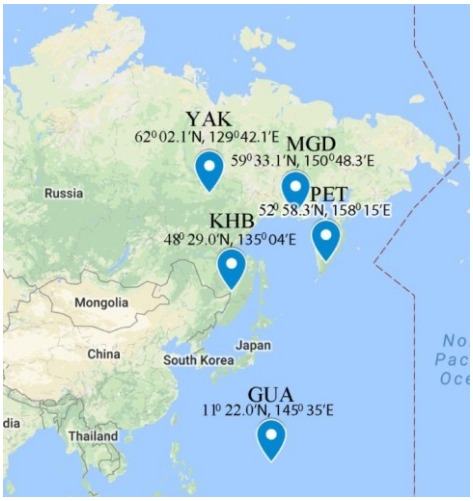

Fig. 1. Geographical position of observatories that provided data used in this study

The first analyzed event on May 27, 2017 (see Figure 2) was caused by a coronal mass ejection of solar matter (CME of May 23, the catalogue of ICMES by I. Richardson and H. Cane, http://www.srl.caltech.edu/ACE/ASC/DATA/level3/icmetable2.htm). On the eve of the storm, the solar wind speed was below the mean and did not exceed 370 km/s [22], the Bz component of the IMF changed within +/- 5 nT. Analysis of the results in Figure 2 shows that on the eve of the event, during the periods of AE index increase on May 26 from 09:50 till 13:00 UT and from 18:00 till 27 May 03:20 UT, weak short-period perturbations of the geomagnetic field were observed at the stations under consideration (operation (5) was used, Figure 2 e). The coincidence of the periods of increased geomagnetic activity (Figure 2 f) at the analyzed stations with the periods of the AE-index increase (Figure 2 c), following the southward turning of IMF Bz component (Figure 2, a), allows us to suggest a connection of the detected geomagnetic perturbations with the non-stationary changes in the interplanetary environment parameters and auroral activity intensification. These results agree with the results of the papers [12, 20-22]. Further on May 27 at 14:40 UT, the Bz component turned to the south and dropped to -8 nT, the solar wind speed increased sharply from 295 to 365 km/s, and short-period perturbations were identified (Figure 2 e) at about 15:35 UT at all geomagnetic stations on the basis of operation (5). They corresponded to the beginning of the magnetic storm (storm sudden commencement).

The initial phase of the storm was accompanied by an increase in the Dst-index from 7 to 41 nT (from 15:00 till 19: 00 UT), and auroral activity (maximum AE 400 nT). During the main phase of the storm (decreasing of Dst to -122 nT and increasing of AE to 1960 nT), on May 27 from 22.00 UT, perturbations of maximum intensity were observed (Figure 2 f) at all the stations under analysis. At the same time, due to the different location of the stations, the perturbation dynamics at each station slightly differed. At the equatorial station GUA, short-period perturbations occurred during the initial and main phases of the magnetic storm. At medium and high latitude stations (YAK, MGD, PET, KHB) they occurred during all phases of the storm and at the moments of their occurrences they correlated with the moments of the AE index maxima. The largest perturbation amplitudes were observed at the northern station YAK. We can also note the correlations of the detected geomagnetic perturbations with the AE-index not only in their occurrence times, but also in their intensities (application of the operation (6), Figure 2 f). The recovery phase lasted for about one more day (the Dst-index returned to the initial value on May 29 at 10:00 UT).

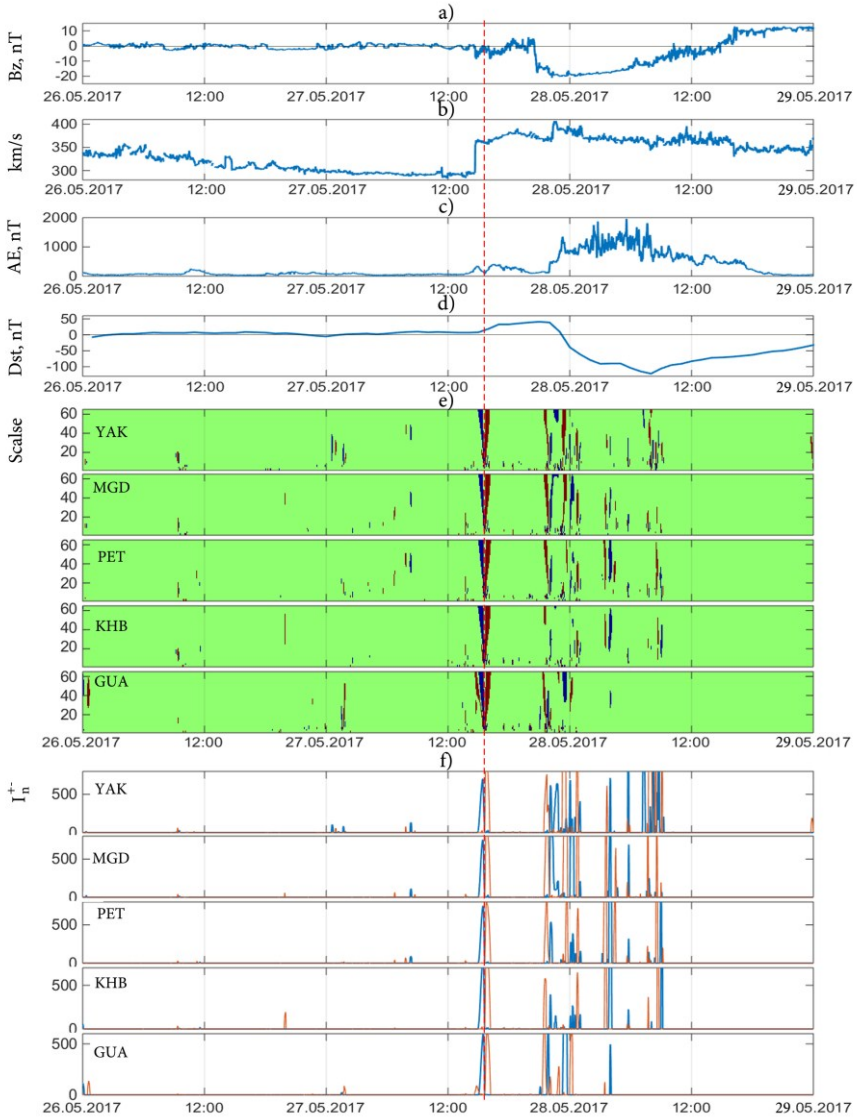

Fig. 2. Processing results of the data for May 15–16, 2017; a) Bz-component of interplanetary magnetic field; b) Speed of solar wind; c) AE-index; d) Dst-index; e) calculations following (5), red color indicates positive perturbations (relative to trend), blue – negative (relative to trend); f) calculations following (6), red color indicates positive perturbation, blue – negative; The vertical dashed line indicates the onset of a magnetic storm

The second analyzed event on July 16, 2017 (see Figure 3) was caused by the CME on July 14 (the catalogue of ICMES by I. Richardson and H. Cane, http://www.srl.caltech.edu/ACE/ASC/DATA/level3/icmetable2.htm). On the eve of the storm, the solar wind speed was below the mean (< 360 km/s) [22], the IMF Bz component changed within +/- 3nT. Analysis of the results of geomagnetic data processing shows that weak geomagnetic disturbances were observed at the analyzed stations on the eve of the event, during AE index increase (Figure 3c) (operation (5) was used, Figure 3 e): on July 15 from 05:00 till 11:00 UT at YAK, MGD, PET stations and on July 16 from 00:40 till 02:25 UT at the all analyzed stations.

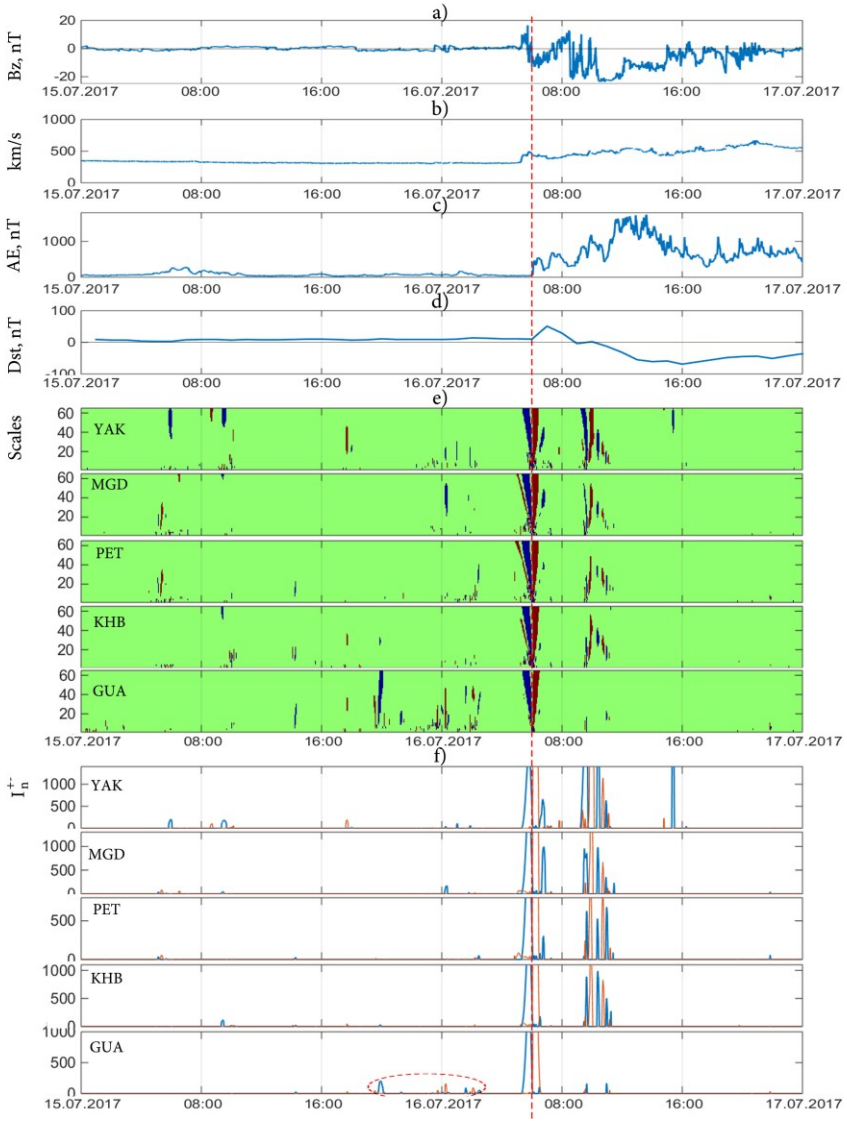

Fig. 3. Processing results of the data for July 26–28, 2017; a) Bz-component of interplanetary magnetic field; b) Speed of solar wind; c) AE-index; d) Dst-index; e) calculations following (5), red color indicates positive perturbations (relative to trend), blue – negative (relative to trend); f) calculations following (6), red color indicates positive perturbation, blue – negative; The vertical dashed line indicates the onset of a magnetic storm

At the beginning of the day on July 16, the Bz-component turned to the north (at 05:15 UT) and rose to the value of 10 nT, the solar wind at this time increased sharply from 340 to 450 km/s. Then at 06:00 UT, short-period perturbations (sudden commencement of the storm) occurred at the stations (Figure 3 e). During the initial phase of the storm, the Dst-index increased to 51 nT (Figure 3 d). The auroral activity also increased to 700 nT (Figure 3 c). Note that during the main phase of the storm, the geomagnetic field variations structure differed at the high-latitude (YAK), mid-latitude (MGD, PET, KHB) and equatorial GUA stations that is probably due to their location. It can also be noted that within a few hours (approximately 10 hours) before the storm, the IMF Bz component

turned to the south and small variations appeared in it (within +/- 4 nT). At the same time, the auroral activity slightly increased (AE-index increased to 110 nT). During the same period, short-term insignificant increases in geomagnetic activity at the equatorial station GUA were observed (the time period in Figure 3 f is shown by dashed lines: on July 15 from 20:00 to 16 June, 02:30 UT). This gives us grounds to assume the connection of the detected perturbations with solar activity and auroral processes.

Table 2 presents the processing results of the data obtained during periods of strong magnetic storms in 2015 and 2017. Processing details of the events on January 7, 2015 and March 17, 2015 are presented in [11-13]. Analysis of the results in Table 2 confirms the possibility of the appearance of weak short-period geomagnetic field perturbations on the eve of magnetic storms.

Table 2. Results of the data processing during magnetic storms, which occurred in 2015

Date of a storm	**Storm source**	**Time of storm beginning (UT)**	**Kp max**	**Dst max**	**AE max**	**Anomalies detected before a magnetic storm**
						Time interval before a magnetic storm beginning
07.01.2015	CME	6:15	6	-103	1327	21 hours
						12 hours 10 minutes
						4 hours 55 minutes
17.03.2015	CME	4:45	8	-233	2250	16 hours 30 minutes
						12 hours 10 minutes
						11 hours 15 minutes
21.06.2015	CIR/CME	16:55	8	-204	2698	10 hours
						7 hours
19.12.2015	CME	16:18	7	-155	1649	25 hours 30 minutes
						15 hours 30 minutes
						7 hours 20 minutes
						1 hour
27.05.2017	CME	15:35	7	-122	1960	28 hours 30 minutes
						14 hours 30 minutes
						2 hours 30 minutes
						1 hour
16.07.2017	CME	6:00	6	-69	1750	24 hours
						20 hours
						11 hours 30 minutes
						3 hours 40 minutes

These results agree with the results of the papers [1, 2] where it was shown that increases in solar wind parameters and the following increases of geomagnetic activity (AE, Kp indices) can be observed prior to abrupt turns of IMF towards south which futher initiate magnetic storms [23].

The possibility of such anomalous effects was also shown earlier in [5, 24] and noted in [15]. This allows us to make an assumption about their solar nature, and determines the applied significance of the study.

4 Conclusions

The processing and analysis of geomagnetic field data from meridianally located stations for the periods of magnetic storms of 2015 and 2017 have been performed. The results of the study showed the general nature of the processes in the analyzed locations. During the periods preceding the beginning of magnetic storms, weak geomagnetic perturbations synchronously appearing at the stations and correlating with the AE-index, both in occurrence times and in intensity, were detected. On the basis of comparison of the results with the interplanetary environment data (the interplanetary magnetic field data and the solar wind parameters were analyzed), with the results of other works [1, 2], we can assume the connection of detected pre-storm geomagnetic perturbations with solar activity and auroral processes. Perturbations of maximum intensity were observed during the main phase of the storm, and the moments of their appearance correlated with the moments of the AE-index maxima. The largest perturbation amplitudes were observed at the northern station YAK.

The results of the experiments showed high sensitivity of the algorithms used and the possibility of its application for a detailed study of the dynamics and spatial-time distribution of geomagnetic disturbances. In the future, the authors plan to continue the study with the increase in statistics and the number of stations analyzed.

Acknowledgements

The research is supported by the grant of the Russian Science Foundation (Project No. 14-11-00194). We would like to thank the staff of geomagnetic observatories at IKIR FEB RAS and at IKFIA SB RAS for providing high quality experimental data. The results presented in this paper rely on the data collected at observatory Guam. We thank USGS for supporting its operation and INTERMAGNET for promoting high standards of magnetic observatory practice (www.intermagnet.org).

References

1. C.J. Davis, M.N. Wild, M. Lockwood, Y.K Tulunay, Ann. Geophysicae, **15**, 217–230 (1997)
2. X.Y. Zhang, M.B. Moldwin, Space Weather, **13**, 130–140 (2015)
3. A.G. Hafez, T.A. Khan, T. Kohda, DIGIT SIGNAL PROCESS, **20(3)**, 715-723 (2010)
4. A. Jach, P. Kokoszka, J. Sojka, L. Zhu, J. Geophys. Res., **111(A9)** doi:10.1029/2006JA011635 (2006)
5. N.A. Barkhatov, V.N. Obridko, S.E. Revunov, S.D. Snegirev, D.V. Shadrukov, O.A. Sheiner, Geomagn. Aeron., **56(2)**, 265–272 (2016)
6. P. Kumar, E. Foufoula-Georgiou, REV GEOPHYS, **35(4)**, 385–412, 1997.
7. V. Klausner, A.R.R. Papa, O. Mendes, M.O. Domingues, P. Frick, JASTP, **92**, 124–136 (2013)
8. Z. Xu, L. Zhu, J. Sojka, P. Kokoszka, A. Jach, J. Atmos. Solar–Terr. Phys., **70,** 1579-1588 (2008)

9. O.V. Mandrikova, I. Solovjev, V.V. Geppenerc, A-KR. Taha, D. Klionskiy, DIGIT SIGNAL PROCESS, **23**, 329–339 (2013)
10. O.V. Mandrikova, S.E. Smirnov, I.S. Solov'ev, Geomagn. Aeron., **52(1)**, 111–120 (2012)
11. O.V. Mandrikova, I.S. Solovev, S.Yu. Khomutov, D.G. Baishev, P. Chandrasekhar, *E3S Web of Conferences*, **20**, 02008 (2017)
12. O.V. Mandrikova, I.S. Solovev, S.Yu. Khomutov, V.V. Geppener, D.M. Klionskiy, M.I. Bogachev, Ann. Geophys., **36**, 1207-1225 (2018)
13. O. Mandrikova, I. Solovev, S. Khomutov, K. Arora, L. Manjula, P. Chandrasekhar, *CEUR Workshop Proceedings*, **1901**, 180-186 (2017)
14. O.V. Mandrikova, I.S. Solovev, T.L. Zalyaev, EPS, **66.** doi:10.1186/s40623-014-0148-0 (2014)
15. O.V. Mandrikova, V.V. Bogdanov, I.S. Solov'ev, Geomagn. Aeron., **53(2)**, 268-273. (2013)
16. O.V. Mandrikova, *Doctoral dissertation*. No. 05200900489 (2009) (in Russian)
17. T.N. Davis, M. Sugiura, I.G.R., **71(3)**, (1966)
18. M. Sugiura, Ann. Int. Geophys., **35**, 9 (1964)
19. E. Thebault, C.C. Finlay, C.D. Beggan, P. Alken, J. Aubert, O. Barrois, F. Bertrand, T. Bondar, A. Boness, L. Brocco, et al., EPS, **67(79)**, (2015)
20. A.N. Zaitsev, P.A. Dalin, G.N.Zastenker, Geomagn. Aeron., **42(6)**, 717-724 (2002)
21. Yu.I. Yermolaev, M.Yu. Yermolaev, IZV ATMOS OCEAN PHY+, **46(7),** 799–819 (2010)
22. W.D. Gonzalez, B.T. Tsurutani, A.L. Clua-Gonzalez, SPAC, **88**, 529–562 (1999)
23. M. Lockwood, M.J. Owens, L.A. Barnard, S. Bentley, C.J. Scott, C.E. Watt, Space Weather, **14**, 406–432 (2016)
24. O.A. Sheiner, V.M. Fridman, Radiophys Quantum El., **54(10)**, 655-666 (2012)